DOI: 10.1002/ejic.201100022

Magnetic and Luminescent Properties of Sm, Eu, Tb, and Dy Coordination Polymers with 2-Hydroxynicotinic Acid

Na Xu,[a] Chao Wang,[a] Wei Shi,[a] Shi-Ping Yan,[a] Peng Cheng,[a] and Dai-Zheng Liao*[a]

Keywords: Lanthanides / Magnetic properties / Coordination polymers

By using multidentate ligand 2-hydroxynicotinic acid (H_2nica), six new lanthanide coordination polymers $[Sm(Hnica)(H_2O)_2SO_4]_n$ (**1**), $\{[Sm_3(Hnica)_6(H_2O)_6(OH)]\cdot 3H_2O\cdot SO_4\}_n$ (**2**), $[Eu(Hnica)(H_2O)_2SO_4]_n$ (**3**), $\{[Eu_3(Hnica)_6(H_2O)_6(OH)]\cdot 6H_2O\cdot SO_4\}_n$ (**4**), $\{[Tb(Hnica)_2(H_2O)_2]ClO_4\cdot H_2O\}_n$ (**5**), and $\{[Dy(Hnica)_2(H_2O)_2]ClO_4\cdot H_2O\}_n$ (**6**) were synthesized and characterized by elemental analysis, IR spectra, and X-ray single-crystal diffraction. Compounds **1** and **3** exhibit a 1D Ln–O–Ln chain structure. Compounds **2** and **4** show a 2D Kagomé lattice structure, whereas **5** and **6** display a 2D rhombic grid structure. The luminescent properties of **1**–**6** at room temperature were studied. Direct-current (dc) magnetic susceptibility studies reveal antiferromagnetic interactions between Ln^{III} ions in **1**–**6**, and alternating-current (ac) magnetic susceptibility data of **6** suggests frequency-dependent out-of-phase signals below 5 K.

Introduction

The design and synthesis of new lanthanide coordination polymers has received much attention not only for their fascinating structures but also their potential applications as luminescent materials, magnetic materials, catalysts, and so on.[1–21] Coordination polymers that contain lanthanide ions such as Sm^{III}, Eu^{III}, Tb^{III}, and Dy^{III} are noteworthy for their sharp transitions in the visible range, so that they are one of the most important components in the pursuit of new luminescent materials.[22] In addition, the nature of the f electron shell of trivalent lanthanides has led to unique magnetic properties. For instance slow relaxation of the magnetization has recently been observed not only in heteronuclear complexes that combine lanthanide ions and other spin centers,[23–29] but also in low-dimensional purely lanthanide-based complexes.[30–39] Therefore lanthanide-based systems are new and important avenues for the exploration of the magnet-like behavior mainly caused by the anisotropy of lanthanide ions. Thus, lanthanide coordination polymers may achieve desired functionality with potential use in a wide range of applications. However, the large ionic radius of lanthanide ions results in high and variable coordination numbers, which make the rational design and synthesis of polymeric lanthanide complexes more difficult than transition-metal ones.[1–3] To some extent, use of rigid multidentate ligands, which help to form steady chelate rings, may overcome this difficulty.[40,41]

2-Hydroxynicotinic acid (H_2nica) contains both carboxyl and hydroxy functional groups that might form six-membered chelate rings with metal ions. By utilizing H_2nica and template agent $(CH_3)_3CCOONa$, we have obtained Pr, Nd, and Gd coordination polymers with structural variations from a 1D chain to 2D layers that show interesting ferro-/antiferromagnetic interactions.[42] Taking into account the intriguing luminescent and/or magnetic properties of Sm^{III}, Eu^{III}, Tb^{III}, and Dy^{III} ions, further studies on H_2nica-based coordination polymers including these Ln^{III} ions are expected. In this contribution, six new coordination polymers, namely, $[Sm(Hnica)(H_2O)_2SO_4]_n$ (**1**), $\{[Sm_3(Hnica)_6(H_2O)_6(OH)]\cdot 3H_2O\cdot SO_4\}_n$ (**2**), $[Eu(Hnica)(H_2O)_2SO_4]_n$ (**3**), $\{[Eu_3(Hnica)_6(H_2O)_6(OH)]\cdot 6H_2O\cdot SO_4\}_n$ (**4**), $\{[Tb(Hnica)_2(H_2O)_2]ClO_4\cdot H_2O\}_n$ (**5**), and $\{[Dy(Hnica)_2(H_2O)_2]ClO_4\cdot H_2O\}_n$ (**6**) were solvothermally synthesized and characterized by means of single-crystal X-ray diffraction analysis. The magnetic studies of **1**–**6** suggested that there were antiferromagnetic interactions in all the complexes; slow relaxation of the magnetization was observed in **6**. The luminescent properties of the six coordination polymers were also studied.

Results and Discussion

The crystal structures of **1** and **3** are isomorphous and exhibit a 1D chain structure. They both crystallize in the monoclinic space group $P2_1/c$. The coordination geometry around the Ln^{III} ion is a slightly distorted monocapped square antiprism, which comprises nine O atoms: O1 from a hydroxy group; O2, O2A, O3A, and O3B from the carb-

[a] Department of Chemistry, Nankai University, Tianjin 300071, P. R. China
E-mail: liaodz@nankai.edu.cn

Supporting information for this article is available on the WWW under http://dx.doi.org/10.1002/ejic.201100022.

oxylic groups of three $Hnica^-$ anions; O6 and O8A from SO_4^{2-} anions; and O4 and O5 from coordinated water molecules (Figure 1, a). Each $Hnica^-$ anion has the same coordination mode, chelates one Ln^{III} ion in the $\eta_{1,1}$ mode, and links to other two adjacent Ln^{III} ions. Thus, every Ln^{III} ion is linked to its neighboring Ln^{III} ions by two monatomic oxygen bridges from the carboxylic groups (Figure 1, b). In the meantime, μ_2-SO_4^{2-} groups alternately link two adjacent Ln^{III} ions. In summary, $Hnica^-$ anions and sulfate groups both bridge the Ln^{III} ions to form an infinite chain, which results in an organic–inorganic hybrid coordination polymer.

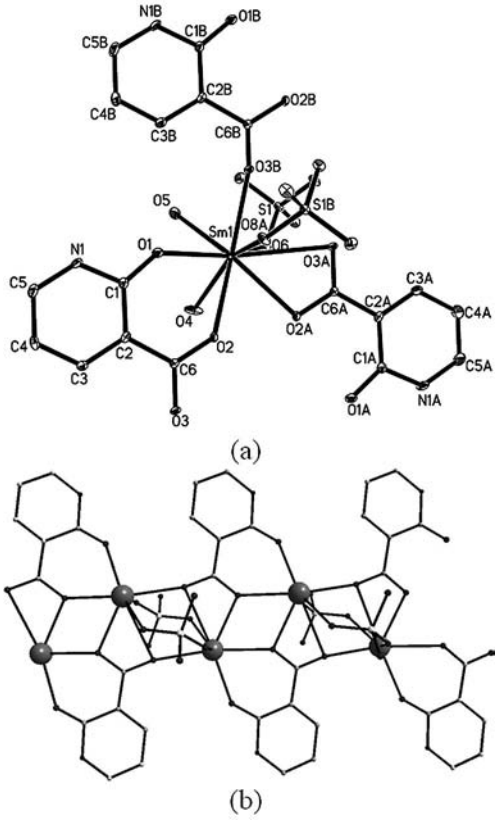

Figure 1. (a) ORTEP plot of $[Sm(Hnica)(H_2O)_2SO_4]_n$ (**1**). Thermal ellipsoids are shown at 30% probability. (b) The 1D chain structure of **1**. All hydrogen atoms and H_2O molecules have been omitted for clarity.

Complexes **2** and **4** both crystallize in trigonal space group $R\bar{3}c$ and display similar 2D layer structures. The Ln^{III} ion lies in a slightly distorted monocapped square-antiprism coordination geometry. O3B and O3C from the hydroxy groups; O1, O1A, O2B, and O2C from the carboxylic groups; and O4, O4A, and O5 (half-occupied) from coordinated H_2O molecules form the coordination sphere (Figure 2, a). The adjacent Ln^{III} ions are linked by $\mu_{1,3}$–COO bridges of the carboxylic groups of $Hnica^-$ and form hexagonal and trigonal metallic rings. Furthermore, the Ln_6 and Ln_3 rings share their edges to form interesting Kagomé 2D lattices (Figure 2, b).

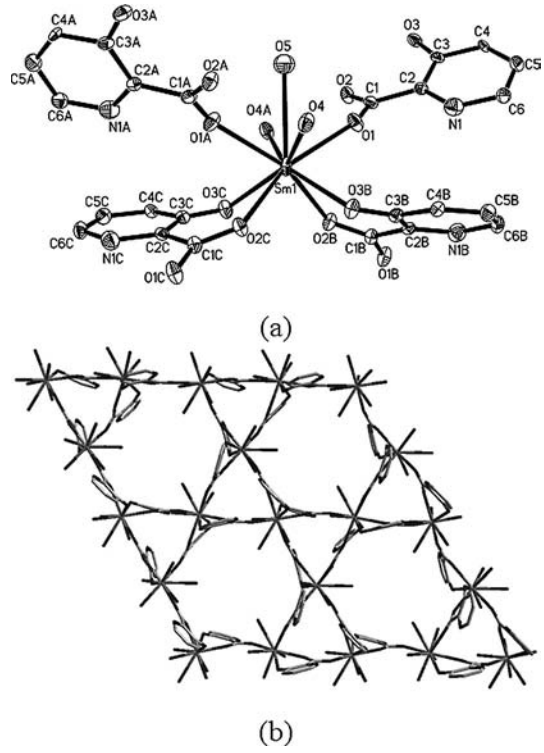

Figure 2. (a) ORTEP plot of $\{[Sm_3(Hnica)_6(H_2O)_6(OH)]\cdot 3H_2O\cdot SO_4\}_n$ (**2**). Thermal ellipsoids are shown at 30% probability. (b) 2D Kagomé lattice structure exhibited by **2**. All hydrogen atoms, guest H_2O molecules, and uncoordinated SO_4^{2-} anions have been omitted for clarity.

We tried to synthesize 2D Kagomé Ln^{III} coordination polymers under different reaction conditions. The pH value is an important factor in the synthesis of lanthanide coordination polymers, but its effect is minor here. Comparison experiments were carried out by using NaOH aqueous solution to take the place of $(CH_3)_3CCOONa$ to adjust the pH to the same values as the synthetic system of 2D Kagomé coordination polymers (**2** or **4**), but 1D coordination polymers (**1** or **3**) were still obtained. This might confirm the template effect of the $(CH_3)_3C$– group in the synthesis of lanthanide coordination polymers with H_2nica.[42]

Complexes **5** and **6** are isomorphous. They both crystallize in the monoclinic space group $P2/c$ and exhibit a 2D lamella structure. There are two kinds of crystallographically independent Ln^{III} ions, both of which lie in a slightly distorted square-antiprism coordination environment (Figure 3, a). Out of the eight oxygen atoms in the coordination sphere of Ln1, four are provided by carboxylic groups (O2, O2A, O5, O5A); and the others are from hydroxy groups (O1, O1A, O4, O4A). For Ln2, the coordination sphere is made of O3, O3B, O6B, and O6C from the carboxylic groups; and O7, O7A, O8, and O8A from coordinated H_2O molecules. Ln1 and Ln2 are linked by $\mu_{1,3}$ carboxylic groups in an alternating way, which results in each Ln1 being related to four Ln2, whereas each Ln2 is related to four Ln1. Thus, Ln1 and Ln2 are linked by carboxylic groups to construct a 2D layer structure composed of rhombic grids (Figure 3, b).

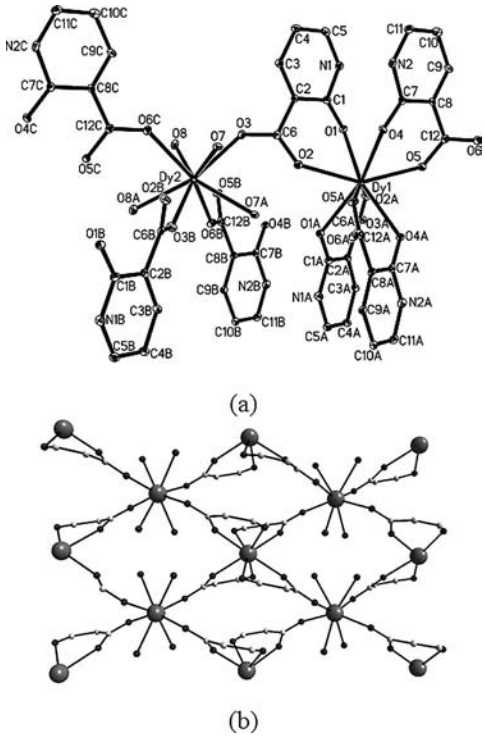

Figure 3. (a) ORTEP plot of $\{[Dy(Hnica)_2(H_2O)_2]ClO_4{\cdot}H_2O\}_n$ (**6**). Thermal ellipsoids are shown at 30% probability. (b) Rhombic grid structure of **6**. All hydrogen atoms, uncoordinated H_2O molecules, ClO_4^- anions, and parts of aromatic rings have been omitted for clarity.

The luminescent properties of **1**–**6** were studied in the solid state at room temperature. The results show that **1**–**6** all exhibit clear characteristic emission spectra of corresponding Sm^{III}, Eu^{III}, Tb^{III}, and Dy^{III} ions as shown in Figure 4. For complexes **1** and **2**, the bands at approximately 562, 598, and 645 nm correspond to the $^4G_{5/2}\rightarrow{}^6H_{5/2}$, $^4G_{5/2}\rightarrow{}^6H_{7/2}$ and $^4G_{5/2}\rightarrow{}^6H_{9/2}$ transitions of Sm^{III}, respectively. For **3** and **4**, the bands at approximately 593, 615, and 699 nm correspond to the $^5D_0\rightarrow{}^7F_1$, $^5D_0\rightarrow{}^7F_2$, and $^5D_0\rightarrow{}^7F_4$ transitions of Eu^{III}, respectively. For **5**, the bands at 490, 545, 585, and 622 nm correspond to the $^5D_4\rightarrow{}^7F_6$, $^5D_4\rightarrow{}^7F_5$, $^5D_4\rightarrow{}^7F_4$, and $^5D_4\rightarrow{}^7F_3$ transitions of Tb^{III}, respectively. For **6**, the bands at 481 and 576 nm correspond to the $^4F_{9/2}\rightarrow{}^6H_{15/2}$ and $^4F_{9/2}\rightarrow{}^6H_{13/2}$ transitions of Dy^{III}, respectively.[43–45]

Magnetic susceptibility measurements of **1**–**6** were performed in a direct-current (dc) field of 1 kOe in the 2–300 K range. They are shown in Figure 5. The $\chi_M T$ values of 0.29 (**1**), 0.31 (**2**), 1.42 (**3**), and 1.49 $cm^3\,K\,mol^{-1}$ (**4**) are much higher than the theoretical values of 0.088 and 0 $cm^3\,K\,mol^{-1}$ for one isolated Sm^{III} ($^6H_{5/2}$, g = 2/7) and Eu^{III} ions ($^7F_0$) in the ground state, respectively, because not just the ground state of these two metal ions but also the first [$^6H^7/_2$ for Sm^{III} and $^7F_1$ for Eu^{III}] and even higher exited states can be populated at room temperature.[46] However, the $\chi_M T$ values of 11.58 (**5**) and 13.75 $cm^3\,K\,mol^{-1}$ (**6**) at 300 K are slightly lower than the theoretical values of 11.81 and 14.13 $cm^3\,K\,mol^{-1}$ for one isolated Tb^{III} ($^7F_6$, g =

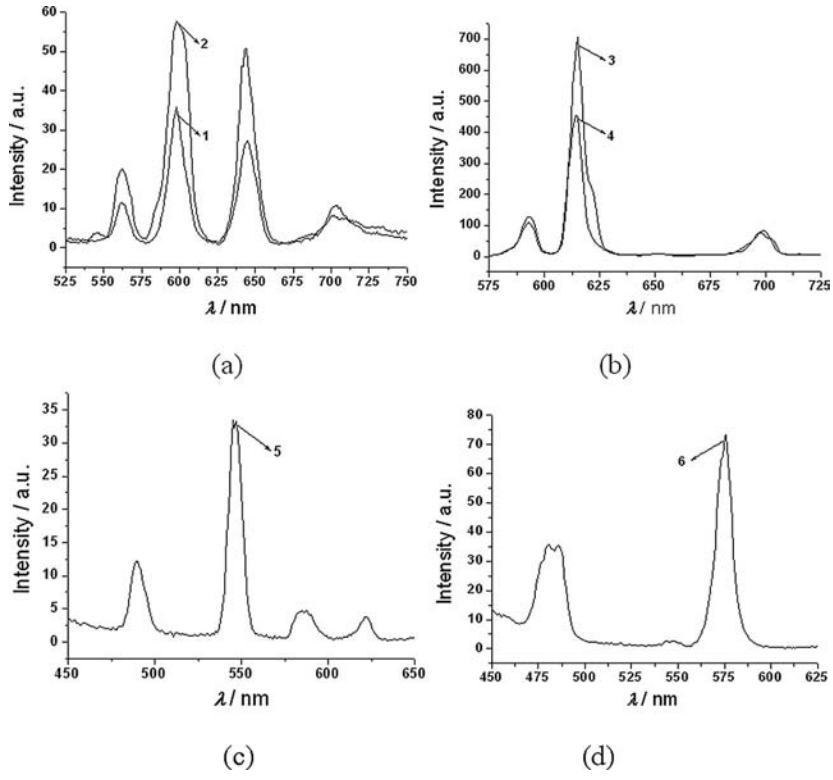

Figure 4. Emission spectra of **1**–**6** in the solid state under the same conditions (excited at 310 nm).

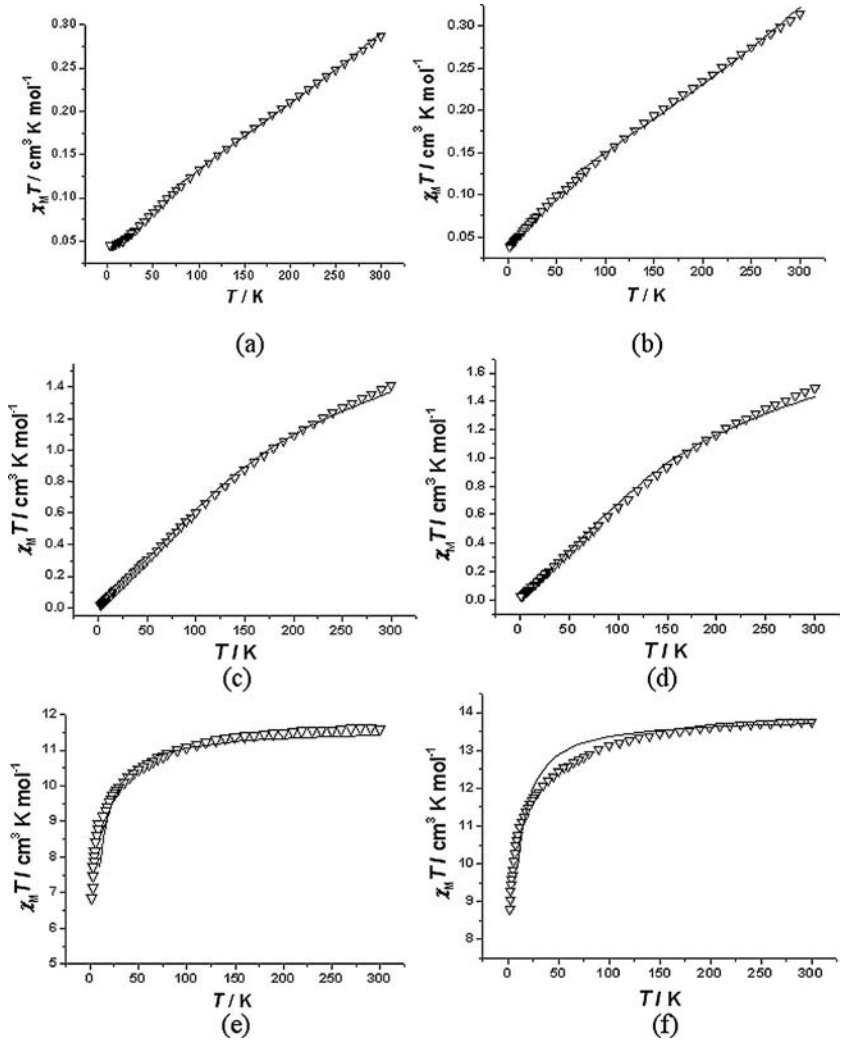

Figure 5. Temperature dependence of $\chi_M T$ for (a) **1**, (b) **2**, (c) **3**, (d) **4**, (e) **5**, and (f) **6** at 1 kOe. The solid lines represent the theoretical values based on the corresponding equations.

3/2) and Dy^{III} ions ($^6H_{15/2}$, g = 4/3) in the ground state, respectively.

For **1** and **2**, the rapid decrease in the $\chi_M T$ values upon lowering the temperature is mainly attributed to the thermal depopulation of the excited levels. The molar magnetic susceptibility can be expressed by Equation (1), which takes into account both the ground state ($^6H_{5/2}$) and the exited states (^6H_J, $J = {}^7/_2, {}^9/_2, {}^{11}/_2, {}^{13}/_2, {}^{15}/_2$) generated by the inter-electronic repulsion and spin–orbit coupling. But Equation (1) is not suitable for the fit in the lower temperature due to the ligand-field effect. For **3** and **4**, upon lowering

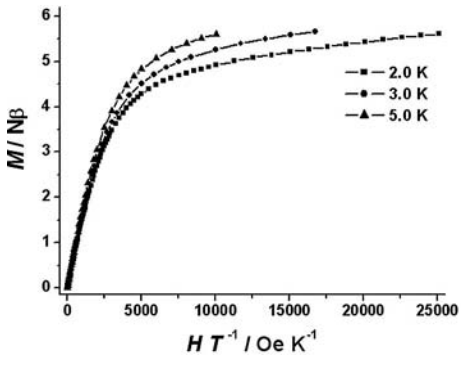

Figure 6. M versus H/T plots at different temperatures below 5.0 K for **6**.

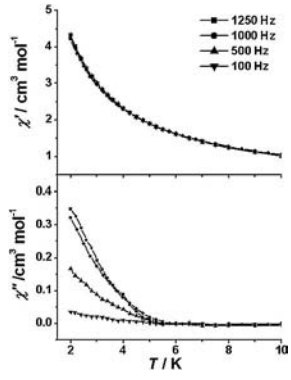

Figure 7. Temperature dependence of the in-phase (top) and out-of-phase (bottom) ac susceptibility for **6** under zero dc field.

the temperature, the $\chi_M T$ values decrease to nearly zero. The molar magnetic susceptibility of **3** and **4** can be reproduced by Equation (2), which also takes into account the contribution both from the ground state ($^7F_0$) and the exited states (^7F_J, J = 0, 1, 2 ... 6).[47] In these expressions, $x = \lambda/kT$, the zJ' parameter based on the molecular-field approximation in Equation (3) is introduced to simulate the magnetic interaction between the Ln^{III} ions;[48] all the other parameters have their usual meanings.

$$\chi_{Sm} = (N\beta^2/3kTx)[2.143x + 7.347 + (42.92x + 1.641)e^{-7x/2} + (283.7x - 0.6571)e^{-8x} + (620.6x - 1.94)e^{-27x/2} + (1122x - 2.835)e^{-20x} + (1813x - 3.556)e^{-55x/2}]/[3 + 4e^{-7x/2} + 5e^{-8x} + 6e^{-27x/2} + 7e^{-20x} + 8e^{-55x/2}] \quad (1)$$

$$\chi_{Eu} = (N\beta^2/3kTx)[24 + (13.5x - 1.5)e^{-x} + (67.5x - 2.5)e^{-3x} + (189x - 3.5)e^{-6x} + (405x - 4.5)e^{-10x} + (742.5x - 5.5)e^{-15x} + (1228.5x - 6.5)e^{-21x}]/[1 + 3e^{-x} + 5e^{-3x} + 7e^{-6x} + 9e^{-10x} + 11e^{-15x} + 13e^{-21x}] \quad (2)$$

$$\chi_{total} = \chi_{Ln}/[1 - (2zJ'/Ng^2\beta^2)\chi_{Ln}] \quad (3)$$

The best fit gives g = 0.27, λ = 268 cm^{-1}, zJ' = –1.54 cm^{-1}, and $R = \Sigma(\chi T_{obsd.} - \chi' T_{calcd.})^2/\Sigma(\chi T_{obsd.})^2$ = 1.28×10^{-4} for **1** in the range of 70–300 K. For compound **2**, the parameters are g = 0.26, λ = 259 cm^{-1}, zJ' = –0.77 cm^{-1}, and $R = 3.47 \times 10^{-4}$ in the range of 70–300 K. For **3**, the parameters are g = 1.95, λ = 336 cm^{-1}, zJ' = –0.01 cm^{-1}, $R = 4.28 \times 10^{-4}$ in the range of 2–300 K. And for **4**, they are g = 2.80, λ = 305 cm^{-1}, zJ' = –0.02 cm^{-1}, and $R = 8.35 \times 10^{-4}$ in the range of 2–300 K (Figure 5). All the above spin–orbit coupling parameters were in accordance with other Sm^{III}/Eu^{III} complexes.[47,49] The negative zJ' values are indicative of the antiferromagnetic interaction between the Ln^{III} ions in these complexes.

For **5** and **6**, the $\chi_M T$ values steadily decrease as T is lowered and reach 6.86 (**5**) and 8.82 $cm^3\,K\,mol^{-1}$ (**6**) at 2 K. To obtain a rough quantitative estimation of the magnetic interaction between Tb^{III} (or Dy^{III}) ions, the Ln^{III} ion could be assumed to exhibit a splitting of the m_j energy levels ($\hat{H} = \Delta\hat{J}_z^2$) in an axial crystal field.[42,50–54] The best-fit parameters are Δ = 0.050 cm^{-1}, zJ' = –0.051 cm^{-1}, g = 1.49, and $R = 6.02 \times 10^{-4}$ for **5** in the range of 2–300 K. For **6**, the parameters are Δ = 0.060 cm^{-1}, zJ' = –0.040 cm^{-1}, g = 1.32, and $R = 5.07 \times 10^{-4}$ in the range of 10–300 K. These results indicate weak antiferromagnetic interactions in **5** and **6**.

Taking into account the intriguing magnetic behavior of the Dy^{III} complex due to the ligand field, which splits the $^6H^{15}/_2$ free ion ground state into eight half-integral Kramers doublets, the magnetic properties for **6** were studied further. As shown in Figure 6, the M versus H/T data below 5.0 K for **6** show a rapid increase of the magnetization at low magnetic field. At higher field, M reaches the value of 5.61 Nβ at 2.0 K and 50 kOe without any sign of saturation of 10 Nβ for one Dy^{III} ion, which is most likely due to the crystal-field effect on the Dy^{III} ions. Furthermore, the non-superposition on the M versus H/T curve at different temperatures implies the presence of low-lying excited states and a significant magnetic anisotropy.[55]

To explore the dynamics of magnetization, ac magnetic measurements of **6** were performed. The zero-field ac susceptibility measurements indicate frequency-dependent out-of-phase signals below 5 K (Figure 7), thus suggesting the onset of slow magnetization relaxation. The ac susceptibility measurements were also performed under 1 kOe applied magnetic field, which led to a shift in the out-of-phase signal to higher temperature (Figure S1 in the Supporting Information) due to fast quantum tunneling suppressed by applying the magnetic field.[25] Unfortunately, the peak of the out-of-phase signal was not detected due to the temperature limitations of the low-temperature apparatus. The origin of slow relaxation of the magnetization is still under question, but the large anisotropy provided by the Dy^{III} ions might play an important role in the phenomenon.

Conclusion

In summary, six lanthanide (Sm, Eu, Tb, and Dy) coordination polymers with 2-hydroxynicotinic acid as ligand have been synthesized under hydrothermal conditions. Compounds **1** and **3** exhibit a Ln–O–Ln 1D chain structure, **2** and **4** show a 2D Kagomé lattice structure, and **5** and **6** display a 2D rhombic grid structure. They all possess good performance in luminescent properties. Weak antiferromagnetic coupling between Ln^{III} centers appears in **1**–**6**. It is worth noting that Dy^{III} complex **6** exhibits frequency-dependent out-of-phase ac signals below 5 K, which suggests the onset of slow magnetization relaxation.

Experimental Section

Materials and Characterization Techniques: All reagents and solvents employed were commercially available and used as received without further purification. Elemental analyses for C, H, and N were performed with a Perkin–Elmer 240 elemental analyzer. The FTIR spectra were measured with a Bruker Tensor 27 spectrometer on KBr disks. The fluorescent spectra were measured with a Varian Cary Eclipse Fluorescence spectrophotometer. Magnetic susceptibilities were measured with a Quantum Design SQUID MPMS XL–7 magnetometer. Diamagnetic corrections were made with Pascal's constants for all the constituent atoms.

$[Sm(Hnica)(H_2O)_2SO_4]_n$ (1): A mixture of H_2nica (0.0834 g, 0.6 mmol), $Sm(NO_3)_3{\cdot}6H_2O$ (0.1778 g, 0.4 mmol), $MnSO_4{\cdot}H_2O$ (0.0676 g, 0.4 mmol), and H_2O (12 mL) was placed in a 25 mL acid digestion bomb and heated at 180 °C for 3 d. Yellow crystals were collected and washed with water (2 × 5 mL) and diethyl ether (2 × 5 mL); yield 0.0807 g, 48% (based on Sm). $C_6H_8NO_9SSm$ (420.54): calcd. C 17.14, H 1.92, N 3.33; found C 16.96, H 1.73, N 3.59. IR (KBr): $\tilde{\nu}$ = 3271 (br), 1633 (vs), 1556 (s), 1519 (s), 1473 (s), 1428 (m), 1392 (m), 1323 (w), 1235 (w), 1120 (s), 911 (w), 784 (w), 608 (m) cm^{-1}.

$\{[Sm_3(Hnica)_6(H_2O)_6(OH)]{\cdot}3H_2O{\cdot}SO_4\}_n$ (2): A mixture of H_2nica (0.0834 g, 0.6 mmol), $Sm(ClO_3)_3{\cdot}6H_2O$ (0.1782 g, 0.32 mmol), $MnSO_4{\cdot}H_2O$ (0.0676 g, 0.4 mmol), $(CH_3)_3CCOONa$ (0.0496 g, 0.4 mmol), and H_2O (12 mL) was placed in a 25 mL acid digestion bomb and heated at 180 °C for 3 d. After a small quantity of precipitates was filtered off, yellow crystals were obtained by slow evaporation of the filtrate at room temperature. The product was

washed with water (2 × 5 mL) and diethyl ether (2 × 5 mL); yield 0.0550 g, 31% (based on Sm). $C_{36}H_{43}N_6O_{32}SSm_3\cdot(H_2O)_6$ (1662.98): calcd. C 26.00, H 3.33, N 5.05; found C 26.05, H 3.24, N 5.19. IR (KBr): $\tilde{\nu}$ = 3082 (br), 1638 (vs), 1558 (s), 1463 (m), 1427 (m), 1382 (s), 1324 (w), 1236 (w), 1110 (s), 787 (m), 662 (w), 572 (w) cm^{-1}.

$[Eu(Hnica)(H_2O)_2SO_4]_n$ (3): Colorless crystals were obtained following a procedure similar to **1** except that $Sm(NO_3)_3\cdot6H_2O$ was replaced by $Eu(NO_3)_3\cdot6H_2O$; yield 0.0777 g, 46% (based on Eu). $C_6H_8EuNO_9S$ (422.15): calcd. C 17.07, H 1.91, N 3.32; found C 16.77, H 1.70, N 3.62. IR (KBr): $\tilde{\nu}$ = 3273 (br), 1634 (vs), 1557 (s), 1520 (s), 1473 (s), 1428 (m), 1392 (m), 1323 (w), 1235 (w), 1119 (s), 911 (w), 783 (w), 609 (m) cm^{-1}.

$\{[Eu_3(Hnica)_6(H_2O)_6(OH)]\cdot6H_2O\cdot SO_4\}_n$ (4): Colorless crystals were obtained following a procedure similar to **2** except that $Sm(ClO_3)_3\cdot6H_2O$ was replaced by $Eu(ClO_3)_3\cdot6H_2O$; yield 0.0534 g, 30% (based on Eu). $C_{36}H_{49}Eu_3N_6O_{35}S(H_2O)_3$ (1667.80): C 25.93, H 3.32, N 5.04; found C 26.05, H 3.25, N 5.19. IR (KBr): $\tilde{\nu}$ = 3081 (br), 1638 (vs), 1558 (s), 1463 (m), 1427 (m), 1382 (s), 1324 (w), 1236 (w), 1110 (s), 788 (m), 662 (w), 572 (w) cm^{-1}.

$\{[Tb(Hnica)_2(H_2O)_2]ClO_4\cdot H_2O\}_n$ (5): Colorless crystals were obtained following a procedure similar to **2** except that $Sm(ClO_3)_3\cdot6H_2O$ was replaced by $Tb(ClO_3)_3\cdot6H_2O$; yield 0.0848 g, 45% (based on Tb). $C_{12}H_{14}ClN_2O_{13}Tb$ (588.62): calcd. C 24.49, H 2.40, N 4.76; found C 24.24, H 2.77, N 4.99. IR (KBr): $\tilde{\nu}$ = 3483 (br), 1638 (vs), 1558 (s), 1475 (m), 1427 (m), 1397 (s), 1326 (w), 1237 (w), 1088 (s), 778 (m), 664 (w), 579 (w) cm^{-1}.

$\{[Dy(Hnica)_2(H_2O)_2]ClO_4\cdot H_2O\}_n$ (6): Yellow crystals were obtained following a procedure similar to **2** except that $Sm(ClO_3)_3\cdot6H_2O$ was replaced by $Dy(ClO_4)_3\cdot6H_2O$; yield 0.0815 g, 43% (based on Dy). $C_{12}H_{14}ClDyN_2O_{13}$ (592.20): calcd. C 24.34, H 2.38, N 4.73; found C 24.41, H 2.41, N 4.55. IR (KBr): $\tilde{\nu}$ = 3284 (br), 1654 (vs), 1558 (s), 1476 (m), 1428 (m), 1398 (s), 1326 (w), 1238 (w), 1088 (s), 778 (m), 665 (w), 579 (w) cm^{-1}.

Crystal Structure Determination: Crystals of **1**–**6** were mounted on glass fibers. Determination of the unit cell and data collection were performed with Mo-K_α radiation (λ = 0.71073 Å) with a Rigaku Saturn 007 diffractometer equipped with a CCD camera. The ω, ϕ scan technique was employed. The structures were solved primarily by direct methods followed by Fourier difference techniques and refined by the full-matrix least-squares method. The computations were performed with the SHELXL–97 program.[56] Non-hydrogen atoms were refined anisotropically. The hydrogen atoms were set in calculated positions and refined as riding atoms with a common fixed isotropic thermal parameter. Crystal data and structure refinements for **1**–**6** are given in Table S1 in the Supporting Information, and the selected bond lengths and angles are listed in Table S2.

CCDC-812605 (for **1**), -812606 (for **2**), -812607 (for **3**), -812608 (for **4**), -812609 (for **5**), and -812610 (for **6**) contain the supplementary crystallographic data for this paper. These data can be obtained free of charge from The Cambridge Crystallographic Data Centre via www.ccdc.cam.ac.uk/data_request/cif.

Supporting Information (see footnote on the first page of this article): Temperature dependence of the out-of-phase susceptibility for **6** measured in the frequency of 1000 Hz under zero and 1 kOe dc field and general information on the X-ray crystallography of **1**–**6** are presented.

Acknowledgments

This work was supported by the National Natural Science Foundation of China (20801028 and 90922032) and the National Basic Research Program of China (973 Program, 2007CB815305).

[1] S. V. Eliseeva, J. C. G. Bünzli, *Chem. Soc. Rev.* **2010**, *39*, 189–227.
[2] J. C. G. Bünzli, S. V. Eliseeva, *J. Rare Earths* **2010**, *28*, 824–842.
[3] B. Valeur, *Molecular Fluorescence: Principles and Applications*, Wiley-VCH, **2001**.
[4] J. C. G. Bünzli, C. Piguet, *Chem. Rev.* **2002**, *102*, 1897–1928.
[5] C. Benelli, D. Gatteschi, *Chem. Rev.* **2002**, *102*, 2369–2387.
[6] A. Y. Robin, K. M. Fromm, *Coord. Chem. Rev.* **2006**, *250*, 2127–2157.
[7] T. M. Reineke, M. Eddaoudi, M. Fehr, D. Kelley, O. M. Yaghi, *J. Am. Chem. Soc.* **1999**, *121*, 1651–1657.
[8] L. Pan, X. Y. Huang, J. Li, Y. G. Wu, N. W. Zheng, *Angew. Chem. Int. Ed.* **2000**, *39*, 527–530.
[9] B. Q. Ma, D. S. Zhang, S. Gao, T. Z. Jin, C. H. Yan, G. X. Xu, *Angew. Chem. Int. Ed.* **2000**, *39*, 3644–3646.
[10] D. L. Long, A. J. Blake, N. R. Champness, C. Wilson, M. Schröder, *Angew. Chem. Int. Ed.* **2001**, *40*, 2444–2447.
[11] D. M. L. Goodgame, D. A. Grachvogel, A. J. P. White, D. J. Williams, *Inorg. Chem.* **2001**, *40*, 6180–6185.
[12] S. J. Dalgarno, C. L. Raston, *Chem. Commun.* **2002**, 2216–2217.
[13] R. Gheorghe, M. Andruh, A. Müller, M. Schmidtmann, *Inorg. Chem.* **2002**, *41*, 5314–5316.
[14] R. Vaidhyanathan, S. Natarajan, C. N. R. Rao, *Inorg. Chem.* **2002**, *41*, 4496–4501.
[15] F. A. Almeida Paz, J. Klinowski, *Chem. Commun.* **2003**, 1484–1485.
[16] S. K. Ghosh, P. K. Bharadwaj, *Inorg. Chem.* **2005**, *44*, 3156–3161.
[17] F. Gándara, A. García-Cortés, C. Cascales, B. Gómez-Lor, E. Gutiérrez-Puebla, M. Iglesias, A. Monge, N. Snejko, *Inorg. Chem.* **2007**, *46*, 3475–3484.
[18] S. N. Semenov, A. Y. Rogachev, S. V. Eliseeva, C. Pettinari, F. Marchetti, A. A. Drozdov, S. I. Troyanov, *Chem. Commun.* **2008**, 1992–1994.
[19] C. Marchal, Y. Filinchuk, X. Y. Chen, D. Imbert, M. Mazzanti, *Chem. Eur. J.* **2009**, *15*, 5273–5288.
[20] G. A. Pereira, J. A. Peters, F. A. Almeida Paz, J. Rocha, C. F. G. C. Geraldes, *Inorg. Chem.* **2010**, *49*, 2969–2947.
[21] M. Koziez, R. Pezka, M. Rams, W. Nitek, B. Sieklucka, *Inorg. Chem.* **2010**, *49*, 4268–4277.
[22] J. C. G. Bünzli, C. Piguet, *Chem. Soc. Rev.* **2005**, *34*, 1048–1077.
[23] L. Bogani, C. Sangregorio, R. Sessoli, D. Gatteschi, *Angew. Chem. Int. Ed.* **2005**, *44*, 5817–5821.
[24] K. Bernot, L. Bogani, A. Caneschi, D. Gatteschi, R. Sessoli, *J. Am. Chem. Soc.* **2006**, *128*, 7947–7956.
[25] N. Lopez, A. V. Prosvirin, H. Zhao, W. Wernsdorfer, K. R. Dunbar, *Chem. Eur. J.* **2009**, *15*, 11390–11400.
[26] S. Osa, T. Kido, N. Matsumoto, N. Re, A. Pochaba, J. Mrozinski, *J. Am. Chem. Soc.* **2004**, *126*, 420–421.
[27] A. Mishra, W. Wernsdorfer, K. A. Abboud, G. Christou, *J. Am. Chem. Soc.* **2004**, *126*, 15648–15649.
[28] F. Mori, T. Nyui, T. Ishida, T. Nogami, K. Y. Choi, H. Nojiri, *J. Am. Chem. Soc.* **2006**, *128*, 1440–1441.
[29] F. Pointillart, K. Bernot, R. Sessoli, D. Gatteschi, *Chem. Eur. J.* **2007**, *13*, 1602–1609.
[30] J. Tang, I. Hewitt, N. T. Madhu, G. Chastanet, W. Wernsdorfer, C. E. Anson, C. Benelli, R. Sessoli, A. K. Powell, *Angew. Chem. Int. Ed.* **2006**, *45*, 1729–1733.
[31] M. T. Gamer, Y. Lan, P. W. Roesky, A. K. Powell, R. Clérac, *Inorg. Chem.* **2008**, *47*, 6581–6583.
[32] H. Ke, G. F. Xu, L. Zhao, J. Tang, X. Y. Zhang, H. J. Zhang, *Chem. Eur. J.* **2009**, *15*, 10335–10338.

[33] P. H. Lin, T. J. Burchell, L. Ungur, L. F. Chibotaru, W. Wernsdorfer, M. Murugesu, *Angew. Chem. Int. Ed.* **2009**, *48*, 9489–9492.
[34] R. Sessoli, A. K. Powell, *Coord. Chem. Rev.* **2009**, *253*, 2328–2341.
[35] N. Ishikawa, M. Sugita, T. Ishikawa, S. Koshihara, Y. Kaizu, *J. Am. Chem. Soc.* **2003**, *125*, 8694–8695.
[36] N. Ishikawa, M. Sugita, W. Wernsdorfer, *Angew. Chem. Int. Ed.* **2005**, *44*, 2931–2935.
[37] N. Ishikawa, M. Sugita, W. Wernsdorfer, *J. Am. Chem. Soc.* **2005**, *127*, 3650–3651.
[38] M. A. AlDamen, J. M. Clemente-Juan, E. Coronado, C. Martí-Gastaldo, A. Gaita-Ariño, *J. Am. Chem. Soc.* **2008**, *130*, 8874–8875.
[39] M. A. AlDamen, S. Cardona-Serra, J. M. Clemente-Juan, E. Coronado, A. Gaita-Ariño, C. Martí-Gastaldo, F. Luis, O. Montero, *Inorg. Chem.* **2009**, *48*, 3467–3479.
[40] N. E. Dean, R. D. Hancock, C. L. Cahill, M. Frisch, *Inorg. Chem.* **2008**, *47*, 2000–2010.
[41] N. R. Kelly, S. Goetz, S. R. Batten, P. E. Kruger, *CrystEngComm* **2008**, *10*, 1018–1026.
[42] N. Xu, W. Shi, D. Z. Liao, S. P. Yan, P. Cheng, *Inorg. Chem.* **2008**, *47*, 8748–8756.
[43] G. Zucchi, R. Scopelliti, J. C. G. Bünzli, *J. Chem. Soc., Dalton Trans.* **2001**, 1975–1985.
[44] G. Vicentini, L. B. Zinner, J. Zukerman-Schpector, K. Zinner, *Coord. Chem. Rev.* **2000**, *196*, 353–382.
[45] C. Tedeschi, J. Azema, H. Gornitzka, P. Tisnes, C. Picard, *Dalton Trans.* **2003**, 1738–1745.
[46] O. Kahn, *Molecular Magnetism*, VCH, New York, **1993**.
[47] M. Andruh, E. Bakalbassis, O. Kahn, J. C. Trombe, P. Porcher, *Inorg. Chem.* **1993**, *32*, 1616–1622.
[48] C. J. O'Connor, *Prog. Inorg. Chem.* **1982**, *29*, 203–283.
[49] Y. Hinatsu, Y. Doi, *Bull. Chem. Soc. Jpn.* **2003**, *76*, 1093–1113.
[50] I. A. Kahwa, J. Selbin, C. J. O'Connor, J. W. Foise, G. L. McPherson, *Inorg. Chim. Acta* **1988**, *148*, 265–272.
[51] J. K. Tang, Q. L. Wang, F. Si-Shu, D. Z. Liao, Z. H. Jiang, S. P. Yan, P. Cheng, *Inorg. Chim. Acta* **2005**, *358*, 325–330.
[52] B. Li, W. Gu, L. Z. Zhang, J. Qu, Z. P. Ma, X. Liu, D. Z. Liao, *Inorg. Chem.* **2006**, *45*, 10425–10427.
[53] Y. Ouyang, W. Zhang, N. Xu, G. F. Xu, D. Z. Liao, K. Yoshimura, S. P. Yan, P. Cheng, *Inorg. Chem.* **2007**, *46*, 8454–8456.
[54] J. X. Xu, Y. Ma, D. Z. Liao, G. F. Xu, J. Tang, C. Wang, N. Zhou, S. P. Yan, P. Cheng, L. C. Li, *Inorg. Chem.* **2009**, *48*, 8890–8896.
[55] P. H. Lin, T. J. Burchell, R. Clerac, M. Murugesu, *Angew. Chem. Int. Ed.* **2008**, *47*, 8848–8851.
[56] G. M. Sheldrick, *Acta Crystallogr., Sect. A: Crystallogr.* **2008**, *64*, 112–122.

Received: January 8, 2011
Published Online: April 7, 2011

